Fatigue fracture behaviour of PEEK: 1. Effects of load level

M. Brillhart, B. L. Gregory and J. Botsis*
Department of Civil Engineering, Mechanics and Metallurgy (m/c 246), University of Illinois at Chicago, Chicago, IL 60680, USA
(Received 26 March 1990; accepted 13 June 1990)

Results of experimental studies on fatigue fracture behaviour of PEEK are reported. Experiments are conducted on injection moulded single edge notched specimens of 2.68 mm in thickness. At low crack speeds the crack tip is relatively round. At relatively higher crack speeds, the crack tip geometry changes to a triangular shape with an angle of 90° which remains constant until close to unstable fracture. Optical microscopy observations of fracture surfaces and of transverse sections show that at relatively short crack lengths growth occurs in a 'brittle' manner. Subsequently necking or lateral contraction of the specimen around the crack tip is observed and is associated with a 'ductile' mode of growth. The point of transition from 'brittle' to 'ductile' fracture is dependent upon the level of the stress. Fatigue striations are observed throughout the fracture surface. Correlation of the striations and the number of cycles indicates a one cycle crack growth mode. The critical crack length is assumed to correspond to the point of minimum thinning which is shortly after the last striation. Hysteretic losses during fatigue crack growth are negligible until a few cycles prior to unstable fracture. Energy release rates evaluated from load displacement curves are practically equal to $J_1 = \delta\sigma_y$ (σ_y is the yield stress of the material and δ is the crack opening displacement). The 'brittle' phase of crack propagation is well described by linear elastic fracture mechanics parameters. For the entire phase of propagation and for the same level of J_1 ($= \delta\sigma_y$), the crack speed is practically independent of the stress level.

(Keywords: polyetheretherketone; fatigue; slip process; ductile fracture)

INTRODUCTION

The requirements mandated by today's structural design needs call for the development of materials that are lightweight, possess relatively higher toughness and are able to withstand a wide variety of aggressive service environments. High temperature thermoplastics and their composites are classes of materials that attempt to satisfy some of the challenging materials requirements.

High temperature thermoplastics such as polyetheretherketone (PEEK) compete with thermosets and thermoplastics in many structural applications. When compared to other synthetic polymers, PEEK exhibits increased fracture toughness and delamination resistance, thermal stability as well as increased resistance to chemical attack and radiation. An additional benefit of PEEK is that it is a thermoplastic. Therefore, *in situ* repairs are possible as opposed to thermosetting materials where removal and replacement are the only maintenance option.

PEEK and its composites possess excellent properties and as such are very promising materials for structural applications. Little is known however, about their fatigue performance. Thus before they can be used in design, the fatigue characteristics of these materials should be thoroughly investigated under a wide spectrum of loading conditions and for a variety of materials structures.

The majority of materials fail by the initiation of a crack which subsequently exhibits slow growth until fracture of the specimen. Furthermore, during fatigue fracture, materials undergo structural transformations (damage) within a relatively small area around the tip of a propagating crack. The extent and intensity of these transformations depend upon the applied load, material type, geometry, processing conditions and corrosion. Damage accumulation, whether in the form of plastic deformation, crazes or voids, is a process that absorbs energy; energy that otherwise would be available to drive the crack. Consequently, an understanding of the various mechanisms of damage nucleation and growth during fracture is essential for the prediction of the life time of structural components and the material toughness.

The physical, mechanical and fracture response of PEEK and its composites have received extensive attention in the last few years[1–9]. Although these studies provide a valuable insight into the behaviour of these materials, investigations of the fatigue fracture behaviour and the underlying mechanisms in PEEK are limited. This is one of a series of papers to report the effects of loading conditions and specimen geometry on fatigue fracture of PEEK. In the first paper, an investigation of the effect of load level on fatigue crack propagation (FCP) is reported. These studies are aimed at the characterization of the macro- and microscopic mechanisms involved during low cycle fatigue conditions of injection moulded single edge notched specimens. Macroscopic studies are concerned with the kinetics of crack propagation, the crack tip morphology and the evolution of the hysteresis load displacement curves. The microscopic studies involve examination of the fracture surfaces, the extent of thinning of the specimen around the crack path and the

* To whom correspondence should be addressed

0032-3861/91/091605-07

location of the critical crack length. Possible effects of processing on the overall fracture behaviour are studied by examination of the fracture surfaces.

EXPERIMENTAL

Specimen preparation

Semicrystalline PEEK 450G used in these studies is provided by ICI (Exton, PA) in the form of 128 × 128 × 3.2 mm injection moulded plaques. The plaques are ground down to approximately 2.68 mm in thickness from both sides in order to remove a layer of amorphous material in the surface region[9]. The depth of the layer is evaluated from optical microscopy observations of sections of the plaques. Single edge notched specimens of 80 mm in gauge length and 25 mm in width are cut from these plaques. A V-shaped notch of 60° and 1 mm in depth is milled into the centre of the gauge length. The specimens are heated in an oven at 140°C for about 3 h and then slowly cooled down to room temperature in the oven. This is intended to remove any moisture that the material could have absorbed during preparation.

Methods

In this study, an MTS dual actuator servohydraulic materials testing system in conjunction with a Wavetech function generator is employed to perform tension–tension fatigue experiments. All experiments are load controlled with a sinusoidal waveform function and conducted under ambient conditions in a laboratory atmosphere.

In all experiments the minimum stress of the fatigue cycle and the frequency are kept constant and at values of $\sigma_{min} = 0$ and $\nu = 0.9$ Hz, respectively, while the levels of σ_{max} are 40.75, 55.15 and 67.80 MPa. These values correspond to load ratio $R = 0$.

Although the frequency is kept constant in all three experiments, the stress rate $\dot{\sigma}$, is different. That is, if $\dot{\sigma}$ is approximated by $\dot{\sigma} = 2\nu(\sigma_{max} - \sigma_{min})$ (ref. 10), the respective stress rates are: 73.35, 99.27 and 122.04 MPa s^{-1}. Therefore, both stress level and stress rate vary from experiment to experiment. However, it is not possible to investigate the effects of stress level while keeping the frequency constant without introducing changes in the stress rate. Conversely, one cannot investigate the effects of stress level having the same stress rate without varying the frequency. Thus, fracture behaviour and the intensity of underlying mechanisms may depend upon the stress level, stress rate and any possible cross effects. Preliminary experimental results indicate a negligible effect of the above range of stress rates on the data reported herein. Work is underway to further elucidate the effects of stress rate on FCP in PEEK[11].

The stress intensity factor K_1 is calculated according to the formula:

$$K_1 = \sigma_{max}(\pi l)^{1/2} f(l/B)$$

Here σ_{max} is the maximum stress, l is the crack length and B is the specimen width. The function $f(l/B)$ is a correction factor related to the specimen geometry and is expressed as[12],

$$f(l/B) = (2B/\pi l \tan \pi l/2B)^{1/2} \times \frac{0.752 + 2.02(l/B) + 0.37(1 - \sin \pi l/2B)^3}{\cos(\pi l/2B)}$$

The elastic energy release rate is calculated as,

$$G_1 = \kappa K_1^2/E$$

Here $\kappa = (1 - \nu^2)$ for plane strain and $\kappa = 1$ for plane stress; E and ν are the Young's modulus and the Poisson's ratio of the material, respectively. It is reported in reference 9 that injection moulded PEEK 450G has a crystallinity of 23%. For that degree of crystallinity, the Young's modulus is about 3 GPa[2]. The Poisson's ratio ν, and the yield stress σ_y, are taken as equal to 0.30 and 91 MPa[13], respectively.

Inasmuch as the ratios of σ_{max}/σ_y are not negligibly small, the following approximation is utilized to calculate crack opening displacements (COD)[14],

$$\delta = K_1^2/E\sigma_y[1 + (\pi^2/24)(\sigma_{max}^2/\sigma_y^2)] \quad (1)$$

(the right hand side of equation (1) is multiplied by 0.6 in the case of plane strain).

Crack growth kinetics and crack opening profiles are recorded on a Hamamatsu video system which is connected to a Questar long range microscope. Load displacement curves are recorded on a Yokogawa plotter. Fracture surfaces are examined on a Zeiss universal optical microscope and on a Jeol scanning electron microscope. Observations on the extent of damage are performed on sections normal to the crack path which are prepared according to standard metallographic grinding and polishing techniques[15].

RESULTS AND DISCUSSION

Crack propagation mechanisms

Figure 1 exhibits a series of optical micrographs of the crack profile taken at the maximum stress of the fatigue cycle. Initially the crack has a relatively round tip. As the crack length increases, the crack tip geometry changes to a triangular shape. The newly formed crack surfaces do not belong to the planes of the crack. However, relaxation takes place within the next cycle, and the newly created surfaces partially contract. This may be due to some viscoelastic behaviour associated with irreversible deformation of the material around the crack tip. Comparison of the bandwidth on the fracture surface and the height of the triangle at the crack tip indicates that they are approximately equal. That is, the crack grows a distance equal to the sliding off at each cycle. Moreover, it is interesting to note that the crack tip angle is about 90° and remains approximately constant until very near the transition to unstable fracture. Similar crack tip geometries have been observed in single crystals of metals and are explained in terms of a 'slipping off' process[16,17]. As a result slip bands emanate from the crack tip. The relatively darker zones (arrows B, *Figure 1*) may be related to slip bands in PEEK. However, it should be noted that the underlying mechanisms of slip at the crack tip might not be the same because PEEK is a semicrystalline material whereas metals are single crystals or polycrystalline.

The evolution of hysteresis loops for the low stress level experiment is shown in *Figure 2*. At the early stages of fatigue fracture the area of the loop is practically insignificant. This indicates that the work spent on irreversible deformation of the test-piece and particularly around the vicinity of the crack tip is negligible. Noticeable hysteresis loops are observed a few cycles

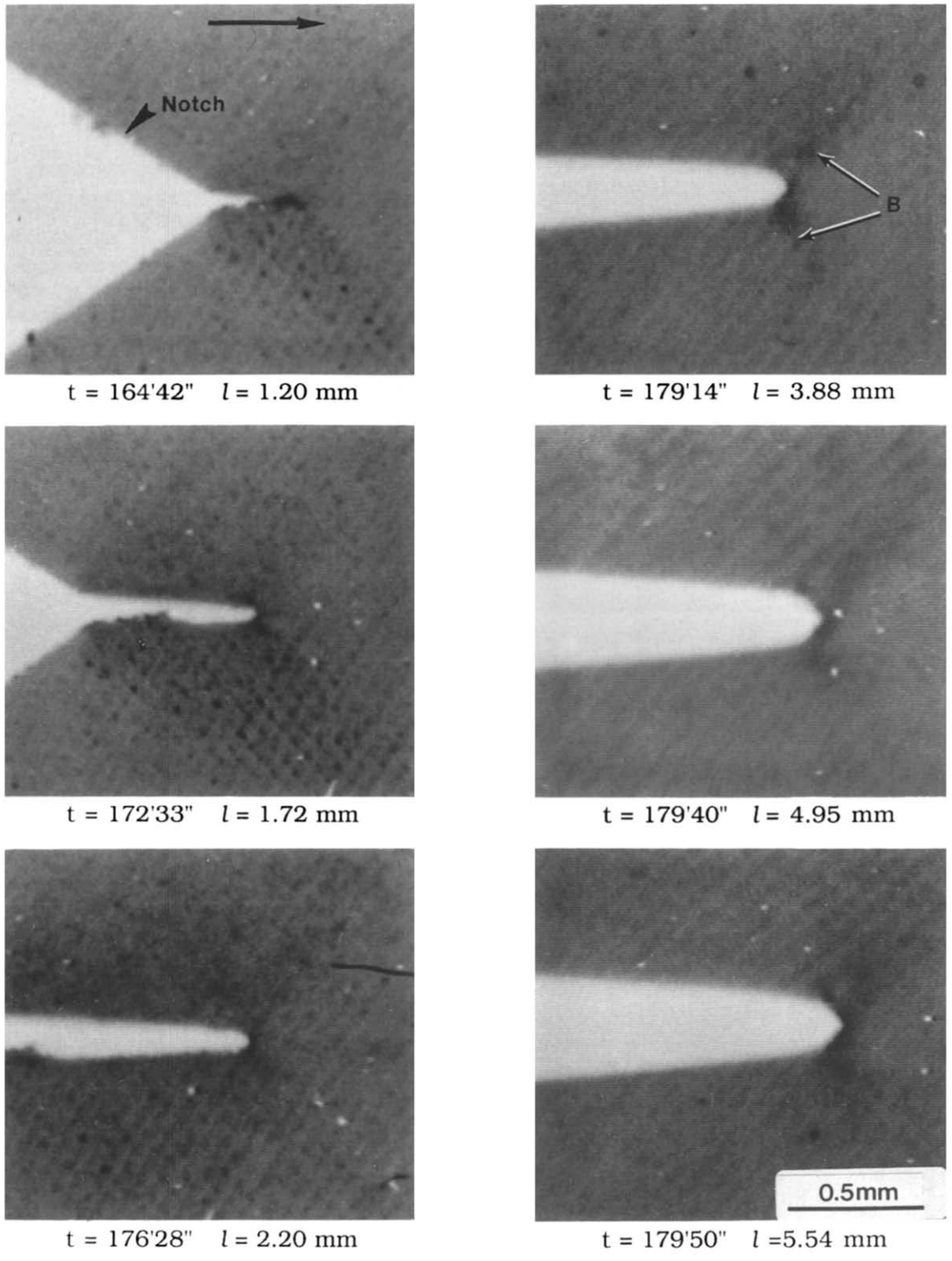

Figure 1 Series of optical micrographs of the crack profile taken at appropriate times and crack lengths. Note the 90° angle of the crack tip in later micrographs. Horizontal arrow indicates the direction of propagation (see text for details)

prior to unstable fracture. This is understood in terms of the relatively large extent of damage around the crack tip at long crack lengths which is manifested in the change of the crack tip geometry (*Figure 1*).

Optical micrographs of the entire fracture surface of three specimens fatigued under three levels of mean stress is shown in *Figure 3*. Clearly, striations appear throughout the slow crack propagation phase. In addition, the striations are bowed in the direction of crack propagation. This may be due to plane strain conditions in the interior and plane stress conditions near the surface of the specimen. Moreover, the injection moulded plaques may have a lower degree of crystallinity near the surface[9] which makes the material more ductile than the interior of the specimen.

The striated morphology of the fracture surface indicates that crack propagation occurs in a discontinuous manner. The size of the bands (i.e. distance between two striations) increases with the crack length. Each band corresponds to a single crack advance. Such an advance

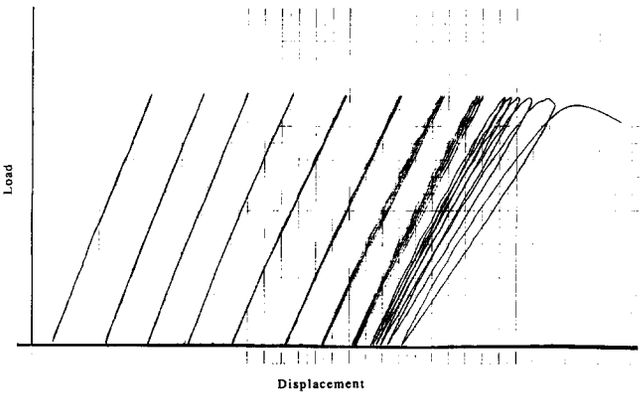

Figure 2 Hysteresis loops for the low stress level experiment (scales: load 0.01 kN mm^{-1}; displacement 0.005 mm mm^{-1})

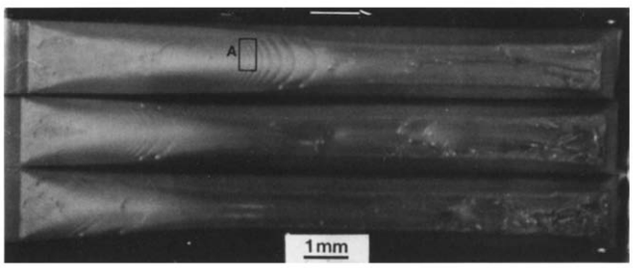

Figure 3 Fracture surfaces of the specimens fatigued under the three different stress levels. Top to bottom: low, middle and high stress levels. Horizontal arrow indicates the direction of propagation

may occur once per many cycles or once per cycle. That is, the crack may remain stationary at a certain crack length for more than one cycle and then jump (within one cycle) to the next configuration, or the crack may jump within every cycle. To examine which mechanism operates in the particular fracture process, we evaluate the following quotients[18]: $\Delta N_c/\Delta l$ and $\Delta N_b/\Delta l$; where ΔN_c and ΔN_b are the increase in the number of cycles and bands, respectively, and Δl is the corresponding crack length increment. Comparison of $\Delta N_c/\Delta l$ and $\Delta N_b/\Delta l$ at each recorded crack length indicates that they are equal. Therefore crack growth occurs with every cycle. Due to this relationship, the fracture surface is a permanent record of the crack speed and can be used to extract crack growth kinetics at relatively fast crack speeds where conventional optical microscope techniques are limited.

To obtain more insight into the type of damage and its extent along directions normal to the crack path, transverse sections of the fractured specimens are examined under an optical microscope. Typical sections are exhibited in *Figure 4*. These micrographs show that at relatively short crack lengths, crack propagation occurs in a 'brittle' manner. When the crack becomes long, localized contraction or necking of the specimen occurs in a zone around the crack tip. This mechanism leads to 'ductile' crack growth and subsequent failure of the test-piece[19,20].

The extent of thinning measured from the fracture surface for three loading conditions is plotted in *Figure 5* as a function of the crack length. Examination of the data shown in *Figure 5* indicates that for every loading condition, thinning reaches a minimum value after the last striation. Furthermore, since striations are formed at the maximum stress of the fatigue cycle, the last striation corresponds to the last completed cycle. Afterwards the specimen is again loaded to nearly the

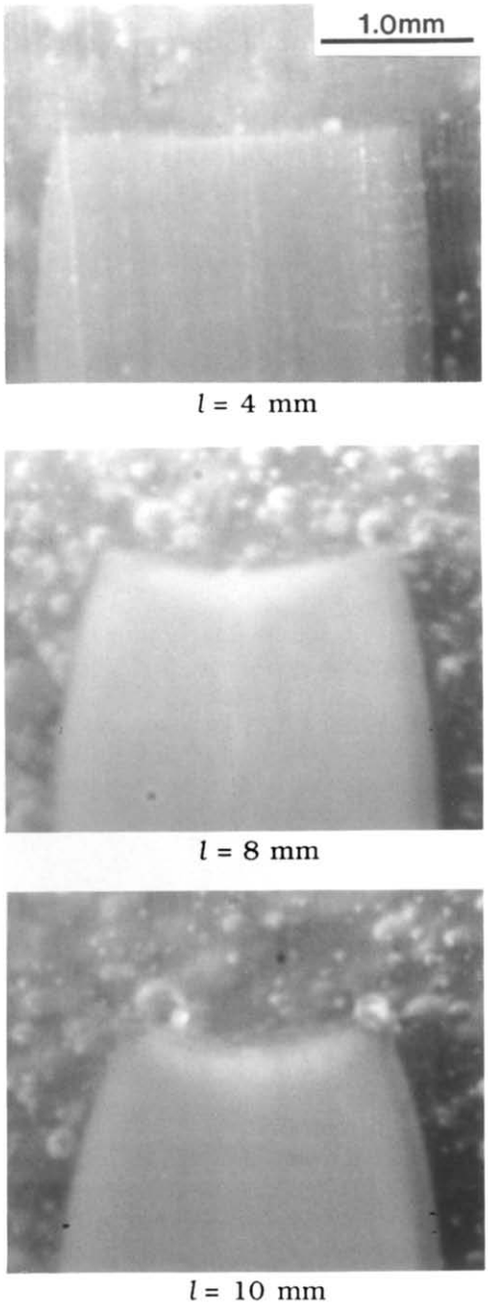

Figure 4 Typical transverse sections of fractured specimens

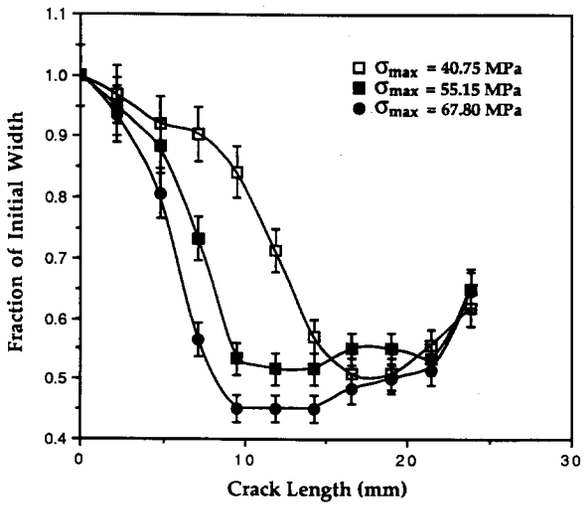

Figure 5 Extent of fracture surface thinning

maximum stress of the fatigue cycle and failure occurs (see *Figure 2*). Evidently, the last striation cannot be taken as the point of transition to fast fracture or for that matter the critical crack length. Therefore it is presumed that the point where minimum thinning occurs corresponds to the transition to fast fracture, i.e. the critical crack length.

The material used in the present studies has been prepared by injection moulding. Due to the finite heat conductivity and complex molecular structure of PEEK a change in morphology may result across the thickness

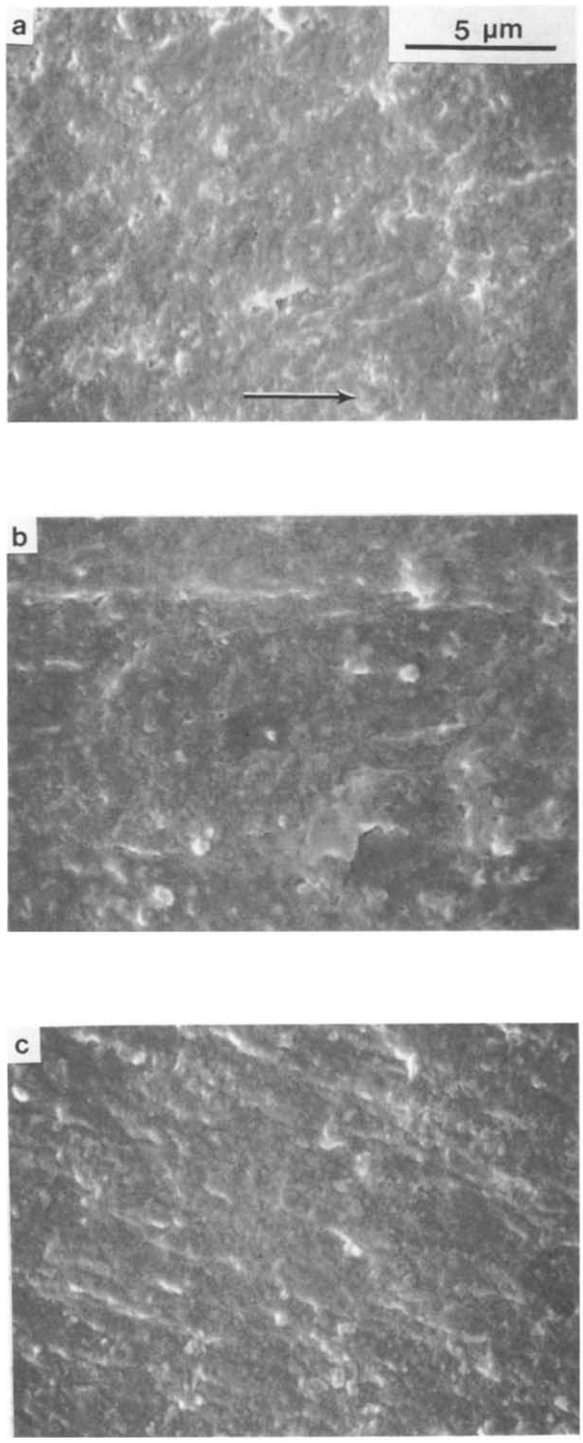

Figure 6 Micrographs of the fracture surface taken at the 'ductile' crack growth region. (a) and (c) have been taken near the edges of the surface and (b) from the middle of the surface

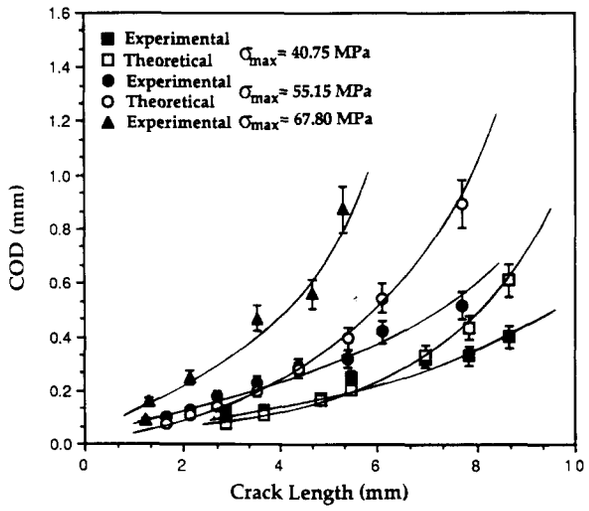

Figure 7 Crack opening displacement plotted against crack length

of the specimen. To investigate effects of such changes on the fracture behaviour, we examine the morphology of the fracture surfaces under an SEM. The micrographs shown in *Figure 6* are taken at the part of the fracture surface where 'ductile' fracture is observed (Box A, *Figure 3*). *Figures 6a* and *6c* are taken near the specimen surfaces and *Figure 6b* at the middle of a fracture surface. Within the resolution of these observations no apparent change in morphology is seen. This may be explained by the fact that the material near the crack planes has been transformed due to extensive irreversible deformation. Thus any structural variations across the thickness have been erased.

Fracture propagation kinetics

The observations described above suggest two modes of fracture: 'brittle' and 'ductile' crack growth. The point of transition is found to be dependent upon the level of stress. Namely, the transition occurs at shorter crack lengths with an increase in stress (*Figure 3*). This is clearly noticed in the experiments with $\sigma_{max} = 40.75$ and 55.15 MPa. In the experiment with $\sigma_{max} = 67.80$ MPa, 'ductile' fracture appears shortly after crack initiation.

The data points in *Figure 7* are experimental values of COD plotted against the crack length for three different stress levels. Linear elastic fracture mechanics (LEFM) parameters may be utilized to describe the COD and crack growth kinetics within the 'brittle' phase of propagation. COD calculated with the use of equation (1) for the middle and low stress level experiments are also shown in *Figure 7*. These data suggest that LEFM can adequately describe the fracture process during the initial phase. A deviation of the calculated (equation 1) and experimental COD is observed in both experiments at crack lengths of about 5.0 mm and 7.0 mm. Similar behaviour is seen in the crack growth kinetics when plotted against the elastic energy release rate G_1. These data are shown in *Figure 8*.

It is difficult to draw on parameters of fracture mechanics in a case of 'ductile' crack growth. Therefore, one should resort to experimentally measured energy release rates and utilize these to correlate FCP data. Values of energy release rates for the low stress level, evaluated from the evolution of load displacement curves are plotted in *Figure 9* as a function of the crack length. Inasmuch as the COD can be readily measured an energy

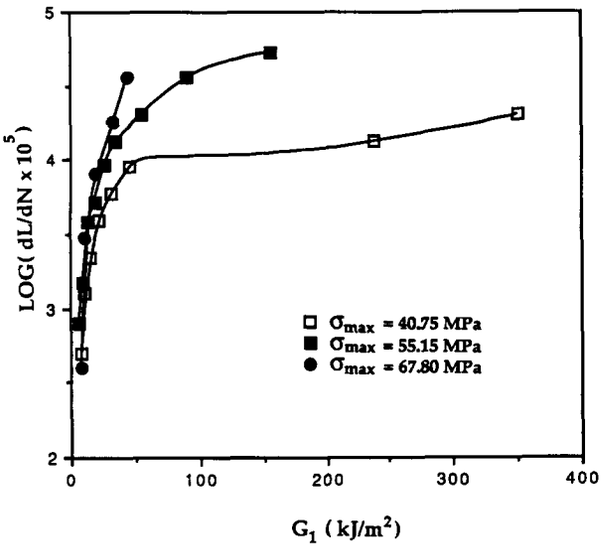

Figure 8 Crack growth kinetics as a function of G_1

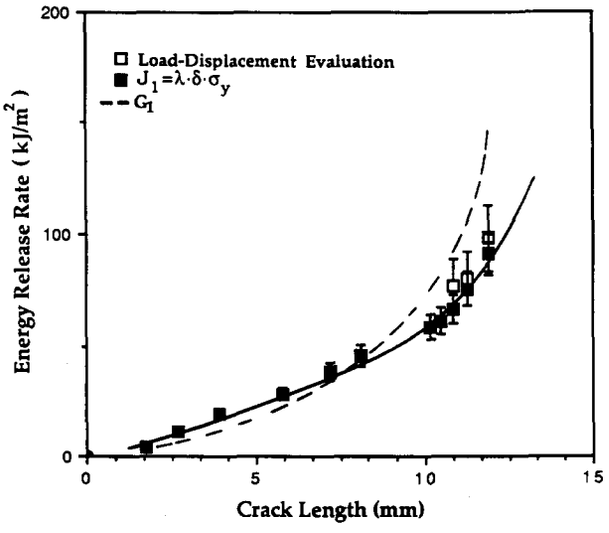

Figure 9 Energy release rates *versus* crack length (see text for details)

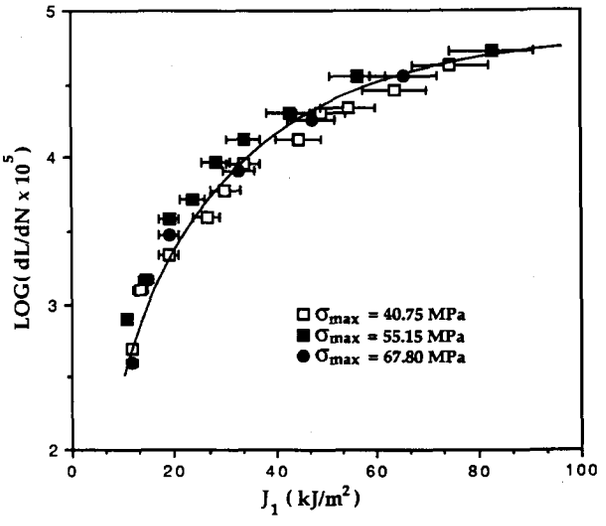

Figure 10 Crack growth kinetics plotted against J_1

release rate $J_1 = \delta\sigma_y$ is computed and shown in *Figure 9*. For comparison the elastic energy release G_1 is also shown in the same figure. It is of interest to note that, in spite of the limitations of J_1 associated with crack growth its values correlate well with the experimentally measured ones. Obviously, G_1 overestimates the actual energy release rate during 'ductile' fracture.

The results shown in *Figure 9* suggest that for the material and the loading conditions used in the present studies, J_1 could be employed to correlate FCP data. Accordingly, one can avoid the laborious and time consuming procedures of generating load displacement curves, especially when a large number of them is required.

The experimental COD shown in *Figure 7* and a yield stress $\sigma_y = 91$ MPa are employed in the evaluation of J_1. The quantities so evaluated are utilized to correlate FCP. For all loading conditions and for the same level of J_1, the kinetic data are practically the same for the entire range of the measurements (*Figure 10*). These results are additional evidence that, in spite of the limitations of J_1 related to crack growth, the actual energy release can be approximated by $J_1 = \delta\sigma_y$ in the studies reported herein.

CONCLUSIONS

The experimental studies of FCP in PEEK presented in this paper show that at the early stages of the process the crack grows in a 'brittle' manner. Subsequently, contraction (necking) of the specimen occurs in a zone around the crack tip. This mechanism leads to a 'ductile' mode of growth. The transition to 'ductile' fracture is dependent upon the stress level. During 'ductile' fracture, the crack profile is triangular with a crack tip angle of 90°. This resembles shapes observed in ductile metals and has been associated with 'slipping off' processes at the crack tip. A single cycle mode of crack growth is observed during slow crack propagation. The 'brittle' phase of crack growth is well described by linear elastic fracture mechanics parameters. The actual energy release rate is approximately equal to $J_1 = \delta\sigma_y$. Crack growth kinetics are practically independent of the stress level when plotted against J_1.

ACKNOWLEDGEMENTS

The authors wish to acknowledge the partial financial support from the FMC Corporation and the Department of Civil Engineering, Mechanics and Metallurgy at the University of Illinois, Chicago. Thanks are also due to Dr A. Fillipov for useful discussions.

REFERENCES

1 Jones, D. P., Leach, D. C. and Moore, D. R. *Polymer* 1985, **26**, 1385
2 Talbot, M. F., Springer, G. S. and Berglund, L. A. *J. Comp. Mater.* 1987, **21**, 1056
3 Lee, L. H., Vanselow, J. and Schneider, S. *Polym. Eng. Sci.* 1988, **28**, 181
4 Lee, Y. and Porter, R. S. *Polym. Eng. Sci.* 1986, **26**, 633
5 Donaldson, S. L. *Composites* 1985, **16**, 103
6 Karger-Kocsis, J. and Friedrich, K. *Polymer* 1986, **27**, 7153
7 Friedrich, K., Walter, R., Voss, H. and Karger-Kocsis, J. *Composites* 1986, **17**, 205
8 Crick, R. A., Leach, D. C., Meakin, P. J. and Moore, D. R. *J. Mater. Sci.* 1987, **22**, 2094

9 Friedrich, K. and Karger-Kocsis, J. in 'Fractography and Failure Mechanisms of Polymers and Composites' (Ed. A. C. Roulin-Moloney), Elsevier Applied Science, London, 1989, p. 437
10 Gregory, B. L. and Botsis, J. *J. Mater. Sci.* 1991, **26**, 1015
11 Gregory, B. L. and Botsis, J. unpublished
12 Tada, H., Paris, P. C. and Irwin, G. P. 'The Stress Analysis of Cracks Handbook', Del Research Corp., Helertown Pennsylvania, 1975, p. 2.11
13 'Modern Plastics Encyclopedia', Vol. 66, McGraw-Hill, New York, 1989
14 Burdekin, F. M. and Stone, D. E. W. *J. Stain Anal.* 1966, **1**, 145
15 Holik, A. S., Kambour, R. P., Fink, D. G. and Hobbs, S. Y. in 'Microstructural Science' (Eds. LeMay, Fallon and McCalls), Elsevier North Holland, Amsterdam, 1979, Vol. 7, p. 357
16 Laird, C. in 'Fatigue and Microstructure', (Ed. M. Meshii), 1978 ASM Materials Science Seminars, ASM, Metals Park, Ohio, 1978, p. 149
17 Neumann, P. *Acta Met.* 1974, **22**, 1155
18 Botsis, J., Chudnovsky, A. and Moet, A. *Int. J. Fract.* 1987, **33**, 263
19 Broek, D. in 'Elementary Fracture Mechanics', 3rd Edn, Martinus Nijhoff, Dordrecht, 1982
20 Hellan, K. in 'Introduction to Fracture Mechanics', McGraw-Hill, New York, 1984